BASIC RESEARCH PAPER

Autophagy 10:6, 972–985; June 2014; © 2014 Landes Bioscience

Small molecule-driven mitophagy-mediated NLRP3 inflammasome inhibition is responsible for the prevention of colitis-associated cancer

Wenjie Guo,[1,2,†] Yang Sun,[1,‡,*] Wen Liu,[1,†] Xingxin Wu,[1] Lele Guo,[1] Peifen Cai,[3] Xuefeng Wu,[1] Xudong Wu,[1] Yan Shen,[1] Yongqian Shu,[3] Yanhong Gu,[3,*] and Qiang Xu[1,*]

[1]State Key Laboratory of Pharmaceutical Biotechnology; School of Life Sciences; Nanjing University; Nanjing, China; [2]School of Pharmacy; Jiangsu University; Zhenjiang, China; [3]Department of Oncology; First Affiliated Hospital of Nanjing Medical University; Nanjing, China

[†]These authors contributed equally to this work.

Keywords: mitophagy, inflammasome, inflammation-associated cancer, colitis, andrographolide

Abbreviations: 3-MA, 3-methyladenine; ACTB, actin, beta; AKT1, v-akt murine thymoma viral oncogene homolog 1; Andro, andrographolide; AOM, azoxymethane; Baf A1, bafilomycin A_1; BECN1, Beclin 1, autophagy-related; BMDM, bone marrow-derived macrophage; CAC, colitis-associated cancer; CARD, caspase recruitment domain; CASP1, caspase 1, apoptosis-related cysteine peptidase; CQ, chloroquine; DAPI, 4′, 6-diamidino-2-phenylindole; DSS, dextran sulfate sodium; EIF4EBP1, eukaryotic translation initiation factor 4E binding protein 1; i.g., intragastrically; i.p., intraperitoneally; IBD, inflammatory bowel disease; IFNG, interferon, gamma; IL1B, interleukin 1, beta; IL6, interleukin 6; IL17A, interleukin 17A; ITGAM/CD11b, integrin, alpha M; MAP1LC3/LC3, microtubule-associated protein 1 light chain 3; MPO, myeloperoxidase; MTOR, mechanistic target of rapamycin; NLRP3, NLR family, pyrin domain containing 3; NSAID, nonsteroidal antiinflammatory drug; PCNA, proliferating cell nuclear antigen; PIK3CA, phosphatidylinositol-4,5-bisphosphate 3-kinase, catalytic subunit alpha; PTGS2/COX2, prostaglandin-endoperoxide synthase 2; PYCARD/ASC, PYD and CARD domain containing; RELA/NFκB p65, v-rel reticuloendotheliosis viral oncogene homolog A; RPS6, ribosomal protein S6; RPS6KB1, ribosomal protein S6 kinase, 70 kDa, polypeptide 1; TNF/TNF-alpha, tumor necrosis factor; TUBA1A, tubulin, alpha 1a; VEGFA, vascular endothelial growth factor A

Nonresolving inflammation in the intestine predisposes individuals to the development of colitis-associated cancer (CAC). Inflammasomes are thought to mediate intestinal homeostasis, and their dysregulation contributes to inflammatory bowel diseases and CAC. However, few agents have been reported to reduce CAC by targeting inflammasomes. Here we show that the small molecule andrographolide (Andro) protects mice against azoxymethane/dextran sulfate sodium-induced colon carcinogenesis through inhibiting the NLRP3 inflammasome. Administration of Andro significantly attenuated colitis progression and tumor burden. Andro also inhibited NLRP3 inflammasome activation in macrophages both in vivo and in vitro, as indicated by reduced expression of cleaved CASP1, disruption of NLRP3-PYCARD-CASP1 complex assembly, and lower IL1B secretion. Importantly, Andro was found to trigger mitophagy in macrophages, leading to a reversed mitochondrial membrane potential collapse, which in turn inactivated the NLRP3 inflammasome. Moreover, downregulation of the PIK3CA-AKT1-MTOR-RPS6KB1 pathway accounted for Andro-induced autophagy. Finally, Andro-driven inhibition of the NLRP3 inflammasome and amelioration of murine models for colitis and CAC were significantly blocked by *BECN1* knockdown, or by various autophagy inhibitors. Taken together, our findings demonstrate that mitophagy-mediated NLRP3 inflammasome inhibition by Andro is responsible for the prevention of CAC. Our data may help guide decisions regarding the use of Andro in patients with inflammatory bowel diseases, which ultimately reduces the risk of CAC.

Introduction

Colorectal cancer is the second leading cause of cancer deaths in the United States and the third most common malignant neoplasm worldwide.[1,2] The development of colorectal cancer is driven by various factors such as genetic mutations, epigenetic abnormalities, and cancer-associated inflammation,[3-6] which has emerged as the seventh hallmark of cancer.[7,8] Studies have shown

*Correspondence to: Yang Sun; Email: yangsun@nju.edu.cn; Qiang Xu; Email: molpharm@163.com; Yanhong Gu; Email: guyhphd@163.com
Submitted: 05/18/2013; Revised: 02/19/2014; Accepted: 02/27/2014; Published Online: 04/01/2014
http://dx.doi.org/10.4161/auto.28374

that the risk of colorectal cancer development in patients with inflammatory bowel diseases (IBD), including ulcerative colitis and Crohn disease, is much higher than that in the general population.[9-12] IBD is thought to result from a breakdown at the epithelial barrier, followed by inappropriate responses to microbial products and chronic inflammation in a genetically susceptible host. The cumulative risk of malignancy can be as high as 40% after 40 y of chronic IBD. Because of the increased risk of colitis-associated cancer (CAC), surveillance colonoscopy has become the standard method to detect dysplasia in individuals with ulcerative colitis. However, it has been estimated that only 20–50% of colonic neoplasms are detected during routine colonoscopy.[13] Therefore, antiinflammatory chemopreventive interventions for this high-risk population are urgently needed.

Inflammasomes are multiprotein complexes that serve as a platform for CASP1/caspase 1 activation and proinflammatory cytokine IL1B (interleukin 1, β) maturation. Thus, inflammasomes have a crucial role in host defense against infection as well as various autoinflammatory conditions.[14] Although a number of inflammasomes have been described, the NLRP3 (NLR family, pyrin domain containing 3) inflammasome is the most extensively studied. Indeed, NLRP3 inflammasome plays an important role in several inflammatory disorders including IBD.[15] NLRP3 inflammasome is triggered by a variety of stimuli, including infection, tissue damage, and metabolic dysregulation, and then activated through an integrated cellular signaling pathway. Many regulatory mechanisms have been identified to attenuate NLRP3 inflammasome signaling at multiple steps. Among them, induction of selective mitochondrial autophagy (known as mitophagy), which results in selective clearance of damaged mitochondria in cells, can negatively regulate NLRP3 inflammasome activation.[16,17] Therefore, a better understanding of the mutual regulation of inflammasomes and autophagy will be essential for discovering new therapeutics for chronic inflammatory diseases.

Andrographolide is a natural diterpenoid that is the major constituent of *Andrographis paniculata*, which is a plant indigenous to Southeast Asian countries that has been used as an herbal medicine in China for thousands of years. Andro has been reported to exert antibacterial, anti-asthmatic, antiviral, and neuroprotective activities,[18-20] and sulfonated Andro (Xi-Yan-Ping Injection) has been approved as a drug for years in China for the treatment of various inflammatory conditions including respiratory infections, bacterial dysentery, and fever. Previously, Andro was reported to inhibit tumor growth in mice at a relatively high dose (about 200 mg/kg),[21] suggesting that a direct antitumor effect might be less involved in its activity. However, the effect of Andro on colitis-associated tumor development has not yet been investigated.

In the present study, we demonstrated that the natural small molecule Andro significantly protected mice against CAC in the mouse model of azoxymethane (AOM)-dextran sulfate sodium (DSS) through inhibiting NLRP3 inflammasome activation in macrophages. Further study showed that Andro triggered mitophagy through inhibiting the PIK3CA-AKT1-MTOR-RPS6KB1 pathway, leading to a reversed mitochondrial membrane potential collapse, which inactivated the NLRP3 inflammasome. The findings obtained in this study suggest that the prevention of CAC results from Andro-driven mitophagy-mediated NLRP3 inflammasome inhibition. Accordingly, these findings may help direct clinical decisions regarding the use of Andro in patients with IBD, ultimately reducing the risk of CAC.

Results

Andro prevents tumorigenesis in a colitis-associated colorectal cancer model

To determine whether Andro directly decreases the incidence of colitis-associated cancer, we generated an AOM-DSS mouse model for colitis-associated colonic tumorigenesis by injecting mice with procarcinogenic AOM followed by 3 cycles of oral DSS administration. Andro was well tolerated, as 100% of the mice survived the treatment. The body weight of the mice was monitored throughout the experiment. The mice lost weight substantially following each exposure to 2.5% DSS and subsequently regained the weight while being maintained on water. In the group of Andro treatment, the mice had a reduced weight loss due to each DSS exposure and recovered more quickly than mice in the AOM-DSS group (**Fig. 1A**). The mice were sacrificed on d 95 following induction. The incidence of tumors was 100% in all mice. However, fewer and smaller tumors were observed in the Andro-treated group (**Fig. 1B and C**). The average number of tumors per mouse in the AOM-DSS group was more than 2 times higher than that in the 15 mg/kg Andro-treated group (**Fig. 1D**). The tumor size was reduced by Andro in a dose-dependent manner (**Fig. 1E and F**). Correspondingly, the average tumor load, which represents the sum of the diameters of all tumors in a given mouse, was significantly decreased in the Andro-treated group (**Fig. 1G**). Moreover, protein expressions of PCNA and p-STAT3 (**Fig. 2A–C**), and mRNA expressions of *Hif1a* and *Vegfa* (**Fig. 2D**) in colonic tissue were remarkably downregulated by Andro treatment. Together, these results indicate that Andro administration reduces colitis-associated tumorigenesis in mice.

Andro attenuates inflammation in a colitis-associated colorectal cancer model

In addition to the reduced colitis-associated tumorigenesis in AOM-DSS-treated mice, we found that the inflammation level was deeply decreased by Andro administration. Phosphorylation of RELA/p65, the subunit of the key inflammatory transcription factor NFKB/NF-κB, was markedly reduced by Andro as shown by immunochemistry and western blotting (**Fig. 2A–C**). Expression of proinflammatory cytokines such as *Tnf/TNF*-α (tumor necrosis factor), *Il17a* (interleukin 17A), and *Il6* (interleukin 6) was also significantly suppressed (**Fig. 2E**). In addition, Andro remarkably inhibited the expression of PTGS2/COX2 (**Fig. 2A and E**), which is an important mediator of the inflammatory process.[22] To determine whether Andro could inhibit tumors that had already formed in the AOM-DSS-induced tumorigenesis model, Andro was given to the mice from d 50 to d 120. Tumors had significantly formed at d 50, and

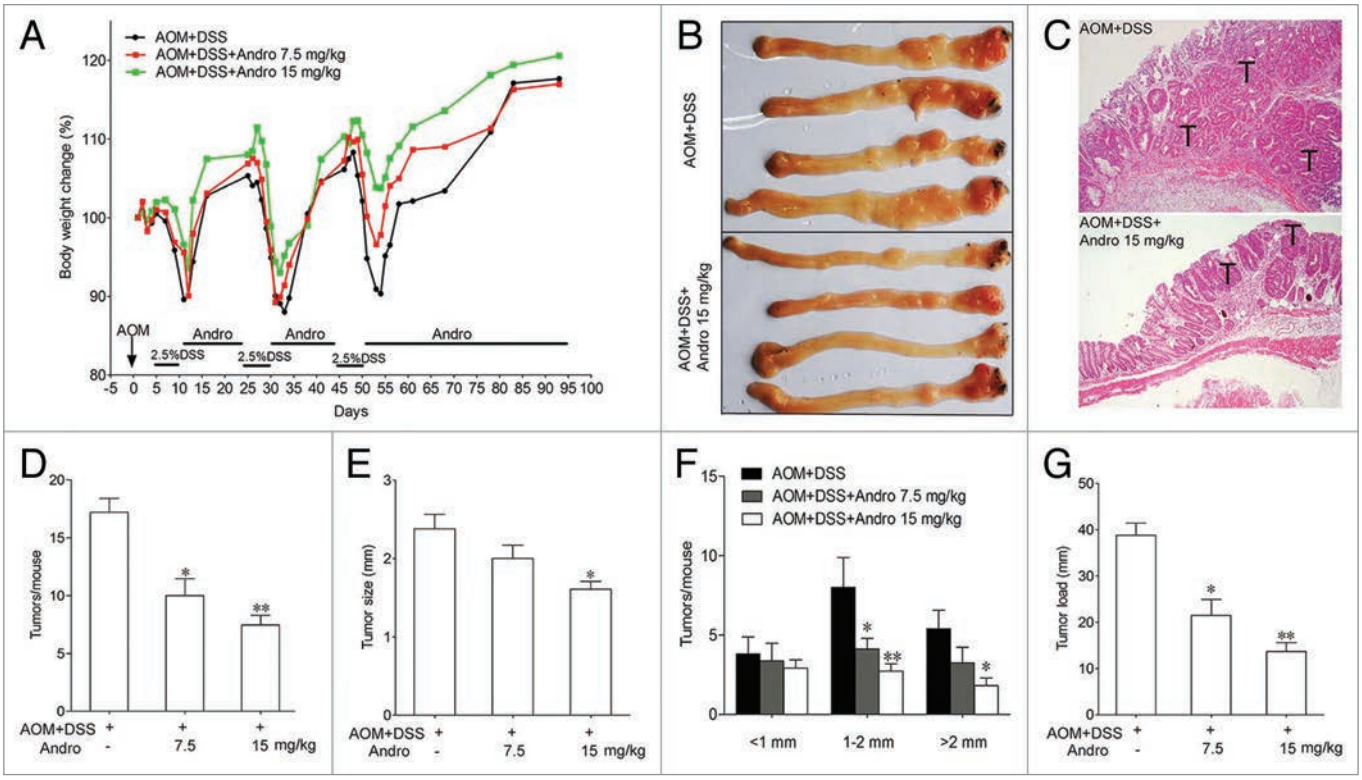

Figure 1. Andrographolide prevents colitis-associated tumorigenesis. Mice were injected i.p. with a single dose (7.5 mg/kg) of AOM followed by 3 cycles of 2.5% DSS given in the drinking water for 5 d. Andro (7.5 and 15 mg/kg) was given i.g. daily during the interval between DSS cycles as shown. Mice were sacrificed on d 95 after CAC induction. (**A**) Body weight was recorded. (**B**) The inside of the colon was photographed. (**C**) Colon tissues were fixed and stained with H&E. (**D**) Tumor numbers were counted. (**E and F**) Tumor diameter and distribution were measured. (**G**) The tumor load was determined by totaling the diameters of all tumors for a given animal. Values are mean ± SEM of 9 mice/group. $^{*}P < 0.05$, $^{**}P < 0.01$ vs. AOM+DSS group. Andro, andrographolide.

Andro given to mice starting at this time point had only a minor effect on tumor growth (**Fig. S1**). Furthermore, we found that Andro at the dose of 15 mg/kg did not inhibit transplanted mouse colon carcinoma CT26 cell growth in mice (**Fig. S2**). Though a previous study reported that Andro inhibited tumor growth, the dose they used was as high as 100–200 mg/kg.[21] Hence, the data obtained here strongly suggest that Andro prevents colitis-associated tumorigenesis by inhibiting inflammation rather than directly killing tumor cells.

Andro ameliorates DSS-induced experimental colitis in mice

Because Andro showed a strong effect in reducing inflammation in the AOM-DSS model, we hypothesized that Andro might prevent tumorigenesis in the AOM-DSS model by inhibiting inflammation. Next, we examined the effect of Andro on DSS-induced experimental colitis in mice. After being challenged with DSS in their drinking water, the mice showed an increasing severity of symptoms, including dramatic body weight loss, rectal bleeding, and diarrhea. Administration of Andro at 2.5 and 5 mg/kg significantly attenuated body weight loss during disease progression, and Andro was more potent than the positive control sulfasalazine administered at a dose of 200 mg/kg (**Fig. 3A**). The disease activity index, which is a clinical parameter that reflects the severity of weight loss, rectal bleeding, and stool consistency, was dose-dependently reduced in the Andro-treated mice relative to the DSS group (**Fig. 3B**). Moreover, Andro alleviated the shortening of the colon caused by DSS treatment (**Fig. 3C and D**). H&E staining and histological analysis revealed severe pathological changes, including mucosal damage, necrosis, and infiltration of inflammatory cells such as neutrophils and monocytes in colon samples of DSS-treated mice. Andro displayed a significant improvement of these pathological changes in a dose-dependent manner (**Fig. 3E and F**). In addition, assessment of myeloperoxidase (MPO) activity in the colons of mice showed a significant suppressive effect of Andro compared with the DSS-treated group (**Fig. 3G**).

Mice with DSS-induced colitis exhibited a cytokine profile similar to that in human IBD, including overproduction of proinflammatory cytokines such as TNF, IL1B, IFNG, and IL17A. The mRNA expression of *Tnf*, *Il1b*, *Ifng*, and *Il17a* and protein expression of TNF, IL1B, IFNG, and IL17A in the colon were remarkably increased after the DSS challenge. Andro significantly suppressed the upregulation of these inflammatory cytokines (**Fig. 3H and I**). NFKB plays an important role in IBD by transcriptional induction of various genes involved in inflammation.[23] We found that Andro treatment markedly reduced the phosphorylation of RELA in

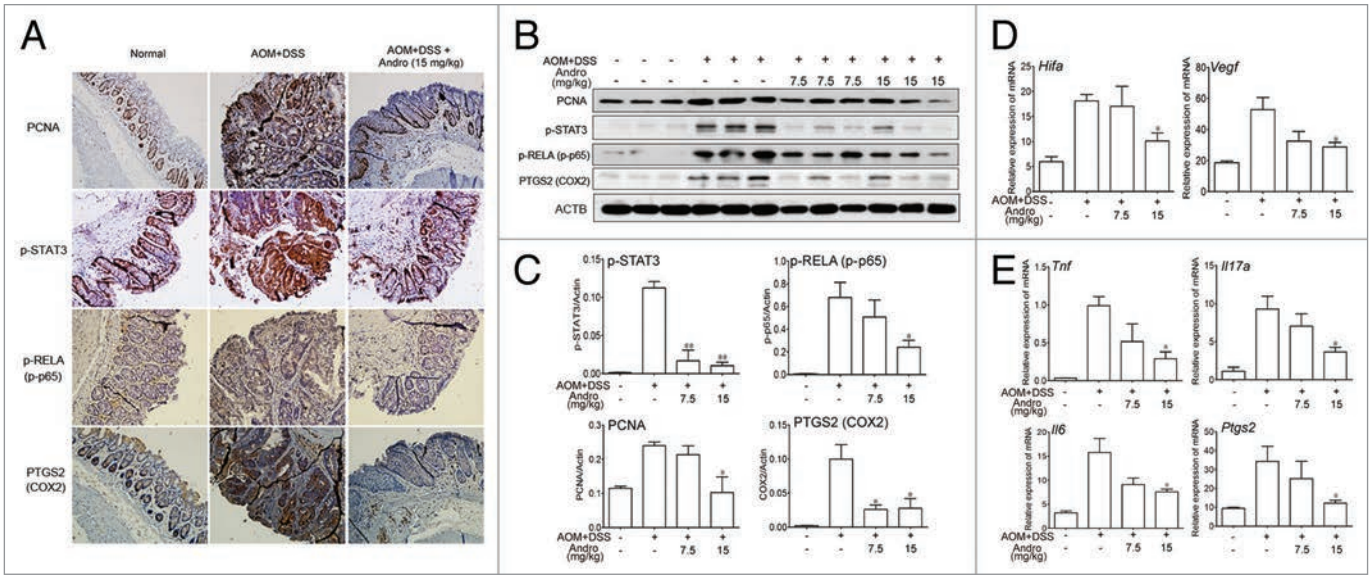

Figure 2. Andrographolide inhibits inflammation in a colitis-associated colorectal cancer model. Mice were subjected to the AOM-DSS model. For other details, see the legend of **Figure 1**. (**A**) The expression of PCNA, p-STAT3, p-RELA/p-p65, and PTGS2/COX2 were analyzed by immunochemistry in paraffin-embedded colon sections. Data shown are representative of 3 experiments. (**B**) The expressions of PCNA, p-STAT3, p-RELA, and PTGS2 in colonic tissues were examined by western blotting. (**C**) Statistical data of the expressions of protein from 3 mice were shown. (**D and E**) The mRNA expressions of *Hif1a*, *Vegfa*, *Tnf*, *Il17a*, *Il6*, and *Ptgs2* in colon sections were determined by real-time PCR. Data are presented as means ± SEM (n = 6). $^{*}P < 0.05$, $^{**}P < 0.01$ vs. AOM+DSS group. Andro, andrographolide.

the colons of DSS-treated mice, as detected by western blotting and immunohistochemistry (**Fig. 3J and K**).

NLRP3 inflammasome inhibition contributes to the antiinflammatory effect of Andro

To investigate the mechanism of Andro-mediated protection from murine colitis, we examined the NLRP3 inflammasome activation in macrophages both in vivo and in vitro. Results from **Figure 4A** showed that Andro treatment (5 mg/kg) prominently inhibited CASP1 activation in vivo as compared with vehicle treatment in DSS-treated mice. In addition, very few infiltrating macrophages were detected in the Andro-treated group (**Fig. 4B**). Next we examined the direct effect of Andro on inflammasome activation in cultured macrophages in vitro. As a result, Andro produced a concentration-dependent inhibition of IL1B secretion from lipopolysaccharide (LPS)-treated human monocytic THP-1 cells and murine bone marrow-derived macrophage (BMDM) by the ELISA assay (**Fig. 5A**) without affecting the survival of macrophages (**Fig. S3**). In addition, detection of the p17 fragment of mature IL1B further confirmed the ELISA results (**Fig. 5B**). Moreover, we found that activation of CASP1 (as indicated by the presence of the cleaved form and enzyme activity) was significantly inhibited by Andro (**Fig. 5B and C**). Furthermore, immunoprecipitation and immunofluorescence analysis showed that the process of NLRP3 inflammasome formation was also interrupted by Andro (**Fig. 5D and E**).

Andro-induced mitophagy is responsible for inhibition of the NLRP3 inflammasome and amelioration of murine models for colitis and CAC

NLRP3 secondary signal activators, such as ATP, induce mitochondrial dysfunction.[24,25] ATP treatment caused mitochondrial damage, as demonstrated by membrane potential collapse (JC-1 staining, **Fig. 6A**), fragmentation (MitoTracker Red staining, **Fig. 7A**) and an abundance of swollen mitochondria with disrupted cristae (transmission electron microscopy, **Fig. 7B**, LPS+ATP group, red arrows). Andro pretreatment prevented ATP-induced collapse of the mitochondria membrane potential (**Fig. 6A**) and mitochondria fragmentation (**Fig. 7A**), as well as swollen mitochondria with cristae disruption (**Fig. 7B**, white arrows). We found that in the Andro-treated group, the damaged mitochondria were localized near a lysosome in the autophagolysosome (**Fig. 7B**, LPS+ATP+Andro group, green arrow) and was surrounded by a double membrane (**Fig. 7B**, LPS+ATP+Andro group, blue arrows), suggesting that Andro triggers mitophagy. In addition, western blot and immunofluorescence staining showed that Andro induced the localization of the phagophore and autophagosomal marker microtubule-associated protein 1 light chain 3/LC3 to mitochondria (**Fig. 6E and F**). These results further suggest that mitophagy is triggered by Andro. To further confirm this phenomenon, we analyzed the expression of LC3. An increase in LC3-labeled vacuole formation in BMDM cells occurred after treatment with 30 μM Andro (**Fig. 6C and F**). Moreover, Andro caused the conversion of LC3-I to LC3-II in a dose- and time-dependent manner in LPS-primed THP-1 cells (**Fig. 6B and D**). Furthermore, we confirmed that Andro inhibited the PIK3CA-AKT1-MTOR-RPS6KB1 pathway (**Fig. 6D**) but had little effect on the MAPK1/ERK2-MAPK3/ERK1-mediated pathway (**Fig. S4**). As expected, Andro-induced inhibition of CASP1 activation and IL1B release was reversed by *BECN1/beclin 1* silencing (**Fig. 8A**) or autophagy inhibitors 3-MA, chloroquine

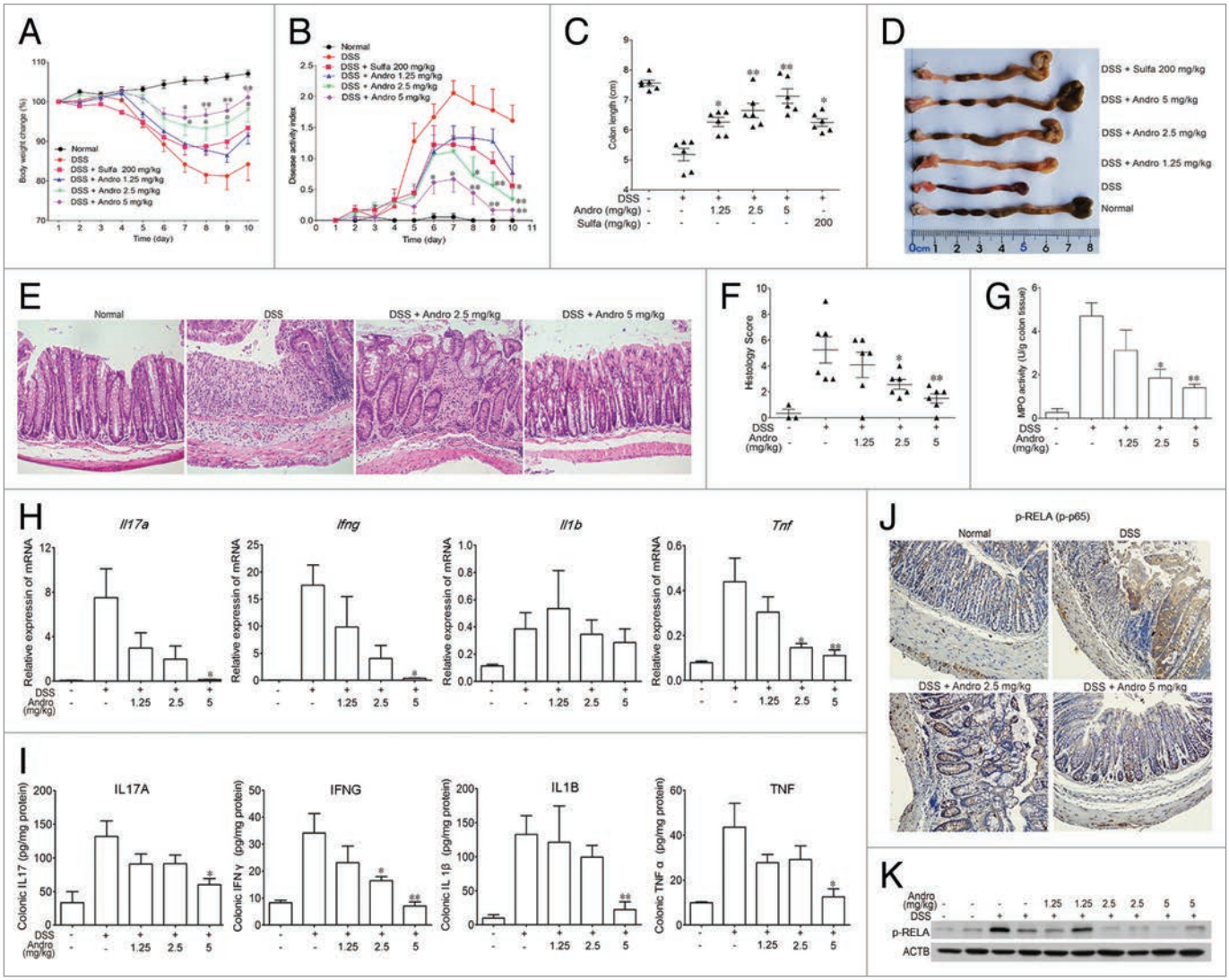

Figure 3. Andrographolide alleviates experimental colitis induced by DSS in mice. Mice were treated with 2.5% DSS in their drinking water for 7 d to induce acute colitis. Andro was administered daily via i.p. injection. Mice were sacrificed on d 10 after colitis induction. (**A**) The body weight of the mice was measured and presented as a percentage of the original body weight. (**B**) The disease activity index was calculated. (**C**) The length of the colon was measured when the mice were sacrificed. (**D**) The colon was photographed. (**E and F**) Paraffin-embedded colon sections were stained with H&E for light microscopy assessment of epithelial damage. (**G**) MPO activity in colonic tissues was detected. (**H**) RNA was extracted from colonic tissues, and mRNA expressions of *Il17a*, *Ifng*, *Il1b*, and *Tnf* were determined by real-time PCR. (**I**) Protein levels of various cytokines in colon homogenates were examined by ELISA. (**J**) Expression of p-RELA was analyzed by immunochemical staining of paraffin-embedded colon sections. (**K**) Expression of p-RELA among colonic proteins was examined by western blotting. Values are mean ± SEM of 6 mice/group. **P* < 0.05, ***P* < 0.01 vs. DSS-treated group. Andro, andrographolide. Sulfa, Sulfasalazine.

(CQ), bafilomycin A_1 (Baf A1), and NH_4Cl (**Fig. 8B and C**). Finally, Andro further enhanced the LC3-II level in cells treated with CQ (**Fig. 8D**), which suggests that the increased autophagic markers (LC3 puncta and LC3-II) in Andro-treated cells are due to increased autophagic flux rather than suppression of the late maturation and degradation stage of autophagy.

To provide evidence linking mitophagy, inflammasomes, and the in vivo outcome of Andro, the autophagy inhibitor CQ was used in the murine models for experimental colitis and CAC to confirm the action of Andro. We found that the ameliorative effect of Andro on murine experimental colitis (**Fig. 9A–E**) and CAC (**Fig. 9F and G**) was significantly blocked by CQ. This blockage was closely related to inhibition of autophagy and aggravation of inflammasome activation (**Fig. 9H and I**). These results strongly support mitophagy as one of the main mechanisms of Andro-mediated inhibition of the NLRP3 inflammasome both in vitro and in vivo.

Discussion

It is now widely accepted that chronic nonresolving inflammation contributes to the initiation, promotion, and progression of tumor development.[26] One of the best clinically

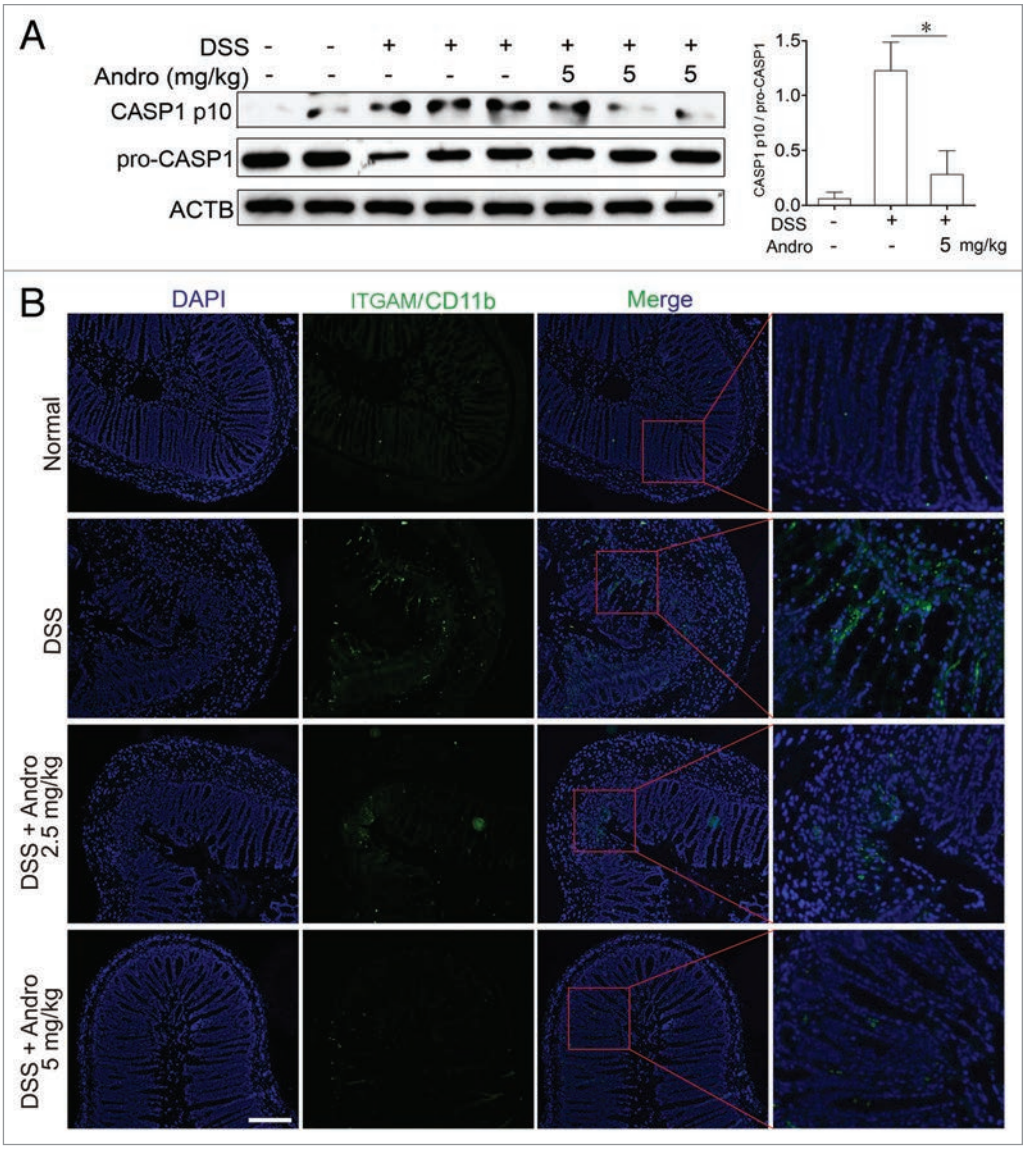

Figure 4. Andrographolide inhibits NLRP3 inflammasome activation in mice with DSS-induced colitis. Mice were treated with 2.5% DSS in their drinking water for 7 d to induce acute colitis. Andro was administered daily via i.p. injection. (**A**) Peritoneal macrophages from mice were isolated on d 7. After stimulation with 5 mM ATP for 30 min, proteins were collected for western blotting. *$P < 0.05$. (**B**) Sections of colonic tissues were immunostained with DAPI (blue) and anti-ITGAM/CD11b-FITC (green) and were observed by fluorescence microscopy. Scale bar: 100 μm. Data shown are representative of 3 experiments. Andro, andrographolide.

characterized examples of the association between inflammation and carcinogenesis is the development of colitis-associated cancer in patients suffering from ulcerative colitis, which is a common form of inflammatory bowel disease.[9] Therefore, new antiinflammatory interventions for the prevention of inflammation-associated cancer are desperately needed.[8,26] We report herein that the small molecule Andro protects mice against CAC by reducing IL1B release from macrophages via mitophagy-mediated NLRP3 inflammmasome inhibition.

Ulcerative colitis is an idiopathic IBD characterized by chronic and recurring inflammation. High levels of the proinflammatory cytokine IL1B secreted by macrophages of the lamina propria from the colon are detected in cases of active colitis and are correlated with the severity of inflammation.[27-31] IL1B modulates the functions of dendritic cells, macrophages, neutrophils, and T cells.[32,33] In particular, IL1B is also involved in the differentiation of Th17 cells.[31,34] IL1B is translated as an inactive 31-kDa precursor (pro-IL1B) after toll-like receptor stimulation (signaling I), and this precursor is cleaved to its activated 17-kDa form by the NLRP3 inflammasome-activated CASP1 (signaling II).[35] Although the NLRP3 inflammasome has been the most extensively studied, our understanding of its function has proven the most elusive.[14] For instance, the role of the NLRP3 inflammasome in colitis and CAC is controversial. Several lines of data from gene-deleted mouse models showed that the NLRP3 inflammasome protects against experimental colitis[36] and colitis-associated tumorigenesis,[37] whereas other groups demonstrated that NLRP3-PYCARD-CASP1-mediated maturation of IL1B is essential for DSS-induced experimental colitis and *nlrp3*$^{-/-}$ mice develop a less severe colitis than wild-type mice.[38-41] Bauer et al. pointed out that these contradictions might result from the different composition of the intestinal microflora.[41] Unlike the controversies resulting from gene-deleted mouse models, IL18 neutralization,[42,43] or chemical CASP1 inhibitor[44,45] treatment effectively reduce severity in murine colitis. Therefore, inhibition of CASP1-mediated IL1B secretion may serve as a useful therapeutic option for patients with IBD.[46,47]

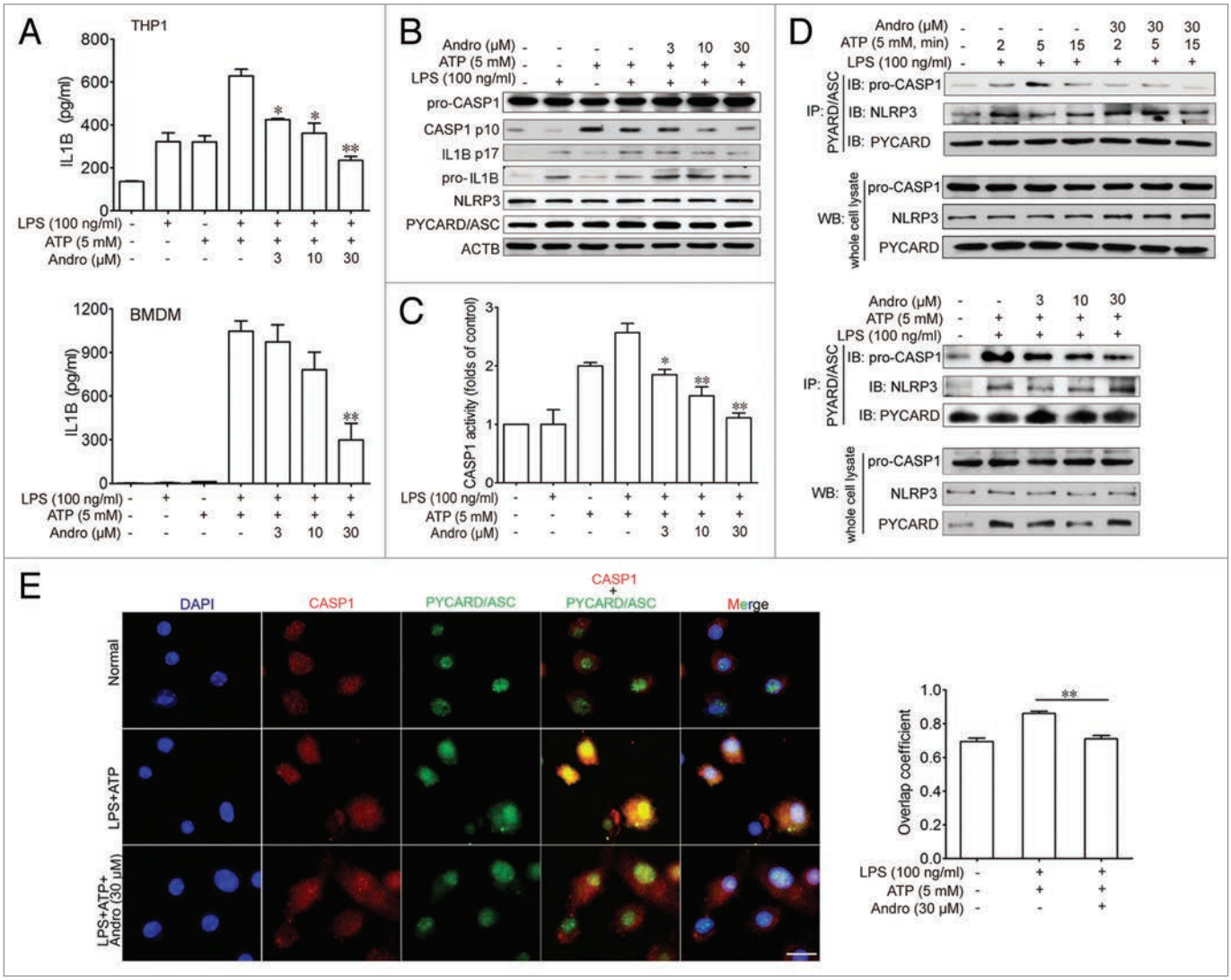

Figure 5. Andrographolide inhibits CASP1 activation and IL1B maturation by interrupting the formation of the NLRP3 inflammasome in vitro. THP-1 (pretreated with 500 nM PMA for 3 h) or BMDM cells were cultured with 100 ng/ml LPS for 3 h, then treated with Andro (3, 10, or 30 μM) for 1 h, followed by 1 h incubation with 5 mM ATP. (**A**) IL1B levels in the supernatant fraction were analyzed by ELISA. Data are mean ± SEM of 3 different experiments. *$P < 0.05$, **$P < 0.01$ vs. LPS+ATP group. (**B**) Protein levels of pro-IL1B, IL1B p17, pro-CASP1, cleaved CASP1, PYCARD, and NRLP3 were determined by western blotting. Data shown are representative of 3 experiments. (**C**) CASP1 activity was measured. Data are mean ± SEM of 3 different experiments. *$P < 0.05$, **$P < 0.01$ vs. LPS+ATP group. (**D**) LPS-primed THP-1 cells were treated with 30 μM Andro for 1 h, followed by 2, 5, or 15 min incubation with 5 mM ATP. In the other experiment, LPS-primed THP-1 cells were treated with Andro (3, 10, or 30 μM) for 1 h, followed by 5 min incubation with 5 mM ATP. Proteins were isolated and immunoprecipitated with an antibody against PYCARD. Data shown are representative of 3 experiments. (**E**) LPS-primed BMDM cells were treated with 30 μM Andro for 1 h, followed by treatment with 5 mM ATP for 15 min. Cells were analyzed by immunofluorescence cytochemistry. Scale bar: 10 μm. Data shown are representative of 3 experiments. Andro, andrographolide.

It has been reported that Andro can decrease IL1B production by affecting signaling I via inhibiting RELA activation.[48,49] Our results also confirmed this inhibitory effect of Andro on phosphorylated RELA in mice with CAC (**Fig. 2A–C**) and with DSS-induced colitis (**Fig. 3J and K**), and in LPS-activated THP-1 cells (**Fig. S5**). In addition to the effect on signaling I, in the present study, we found that Andro disrupted signaling II and inhibited CASP1 activation (**Fig. 4A**; **Fig. 5C and D**), which resulted in a reduction of IL1B secretion in vivo (**Fig. 3I**) and in vitro (**Fig. 5A and B**). CASP1 activation is tightly controlled by signaling II. When activated by diverse stimuli such as signaling from mitochondria (e.g., reactive oxygen species and mitochondrial DNA),[50,51] NLRP3 proteins polymerize and bind to the PYCARD adaptor, which promotes the recruitment of pro-CASP1 through CARD-CARD interactions. Pro-CASP1 then clusters and autocleaves to form the activated CASP1 p10-p20 tetramer, which triggers CASP1-dependent processing of pro-IL1B and pro-IL18.[24,25,52] Because of the negative regulatory role of mitophagy in the NLRP3 inflammasome activation,[24,25,50] mitochondria become a useful target for inflammation control. Our study found that Andro treatment effectively prevented ATP-induced collapse of the mitochondrial

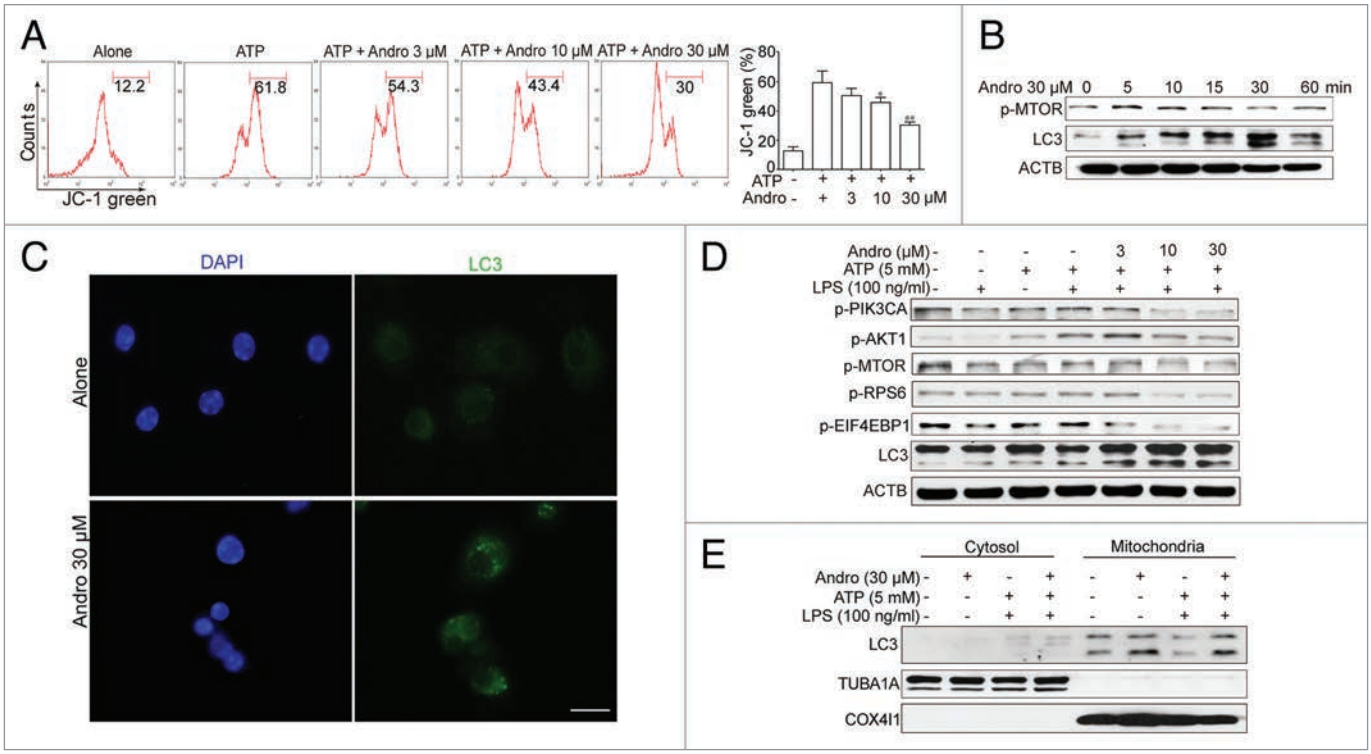

Figure 6. Andrographolide promotes mitophagy and inhibits NLRP3 inflammasome activation in macrophages. (**A**) THP-1 cells, pretreated with 500 nM PMA for 3 h, were cultured with 100 ng/ml LPS for 3 h (below referred to as LPS-primed THP-1 cells), then cells were treated with Andro (3, 10, or 30 μM) for 1 h, followed by 1 h incubation with 5 mM ATP. The mitochondrial membrane potential was determined by JC-1 staining. $^{*}P < 0.05$, $^{**}P < 0.01$ vs. ATP group. (**B**) LPS-primed THP-1 cells were treated with 30 μM Andro for the indicated times. Proteins were collected and the expression of p-MTOR and LC3 was detected by western blot. (**C**) BMDM cells were cultured with 100 ng/ml LPS for 3 h, and then cells were treated with 30 μM Andro for 1 h. LC3-II dot formation was detected by immunofluorescence. Scale bar: 10 μm. (**D**) LPS-primed THP-1 cells were treated with Andro (3, 10, or 30 μM) for 1 h, followed by 1 h incubation with 5 mM ATP. Then proteins were collected and analyzed by western blotting. (**E**) LPS-primed THP-1 cells were treated with 30 μM Andro for 1 h, followed by 1 h incubation with 5 mM ATP. Then mitochondria and cytosol were separated using a commercial kit and detected for LC3 expression. Data shown in (**A**) are mean ± SEM of 3 different experiments. Data shown in (**B–E**) are representative of 3 experiments. Andro, andrographolide.

membrane potential (**Fig. 6A**). Given that autophagy regulated NLRP3-dependent inflammation by preserving mitochondrial integrity,[53] we found that Andro triggered mitophagy through the PIK3CA-AKT1-MTOR-RPS6KB1 pathway (**Fig. 6D**), thereby inhibiting CASP1 activation. But still the detailed molecular mechanisms for Andro's effect on mitophagy remain to be further investigated.

Previous studies suggested that NLRP3 inflammasome activity was negatively regulated by mitophagy and positively regulated by reactive oxygen species.[25] Here we show that Andro-driven mitophagy leads to the reduction of damaged mitochondria, which in turn inactivates the NLRP3 inflammasome and ameliorates colitis and CAC in mice. Our conclusions were based on the following observations: First, Andro-mediated inhibition of CASP1 activation and IL1B release in macrophages was significantly blocked by *BECN1* silencing (**Fig. 8A**) or by the autophagy inhibitors 3-MA, CQ, Baf A1, and NH_4Cl (**Fig. 8B and C**) in vitro. Second, the autophagy inhibitor CQ remarkably abolished the ameliorative effect of Andro on DSS-induced colitis (**Fig. 9A–E**) and AOM-DSS-induced CAC (**Fig. 9F and G**) in mice through inhibiting autophagy. Finally, Andro-induced inhibition of IL1B secretion (**Fig. 9D**) and NLRP3 inflammasome activity (**Fig. 9H and I**) in macrophages was also reversed by CQ treatment in vivo. These data strongly suggest that andrographolide-driven mitophagy-mediated inhibition of the NLRP3 inflammasome is responsible for the amelioration of experimental colitis and colitis-associated tumorigenesis in mice. Together with the data on RELA as shown in **Figure 2**, **Figure 3**, and **Figure S5**, we conclude that the inhibition of both signaling I (one of the NFKB functions) and signaling II of the inflammasome pathway is important for the effects of Andro on colitis and CAC. It should be emphasized that there are few reports on the mitophagy-mediated inhibition of the NLRP3 inflammasome by a small molecule. The effect of Andro reported here is distinct from other known antiinflammatory drugs, such as nonsteroidal antiinflammatory drugs (NSAIDs), which may provide a new choice for the treatment of colitis and its related cancers.

Recently, Andro has been reported to induce autophagic cell death in liver cancer Huh-7 cells through the disruption of the mitochondrial transmembrane potential and elevation of reactive oxygen species.[54] Conversely, Zhou et al. reported that Andro sensitized human cancer cells to cisplatin-induced apoptosis via suppression of autophagosome-lysosome fusion.[55]

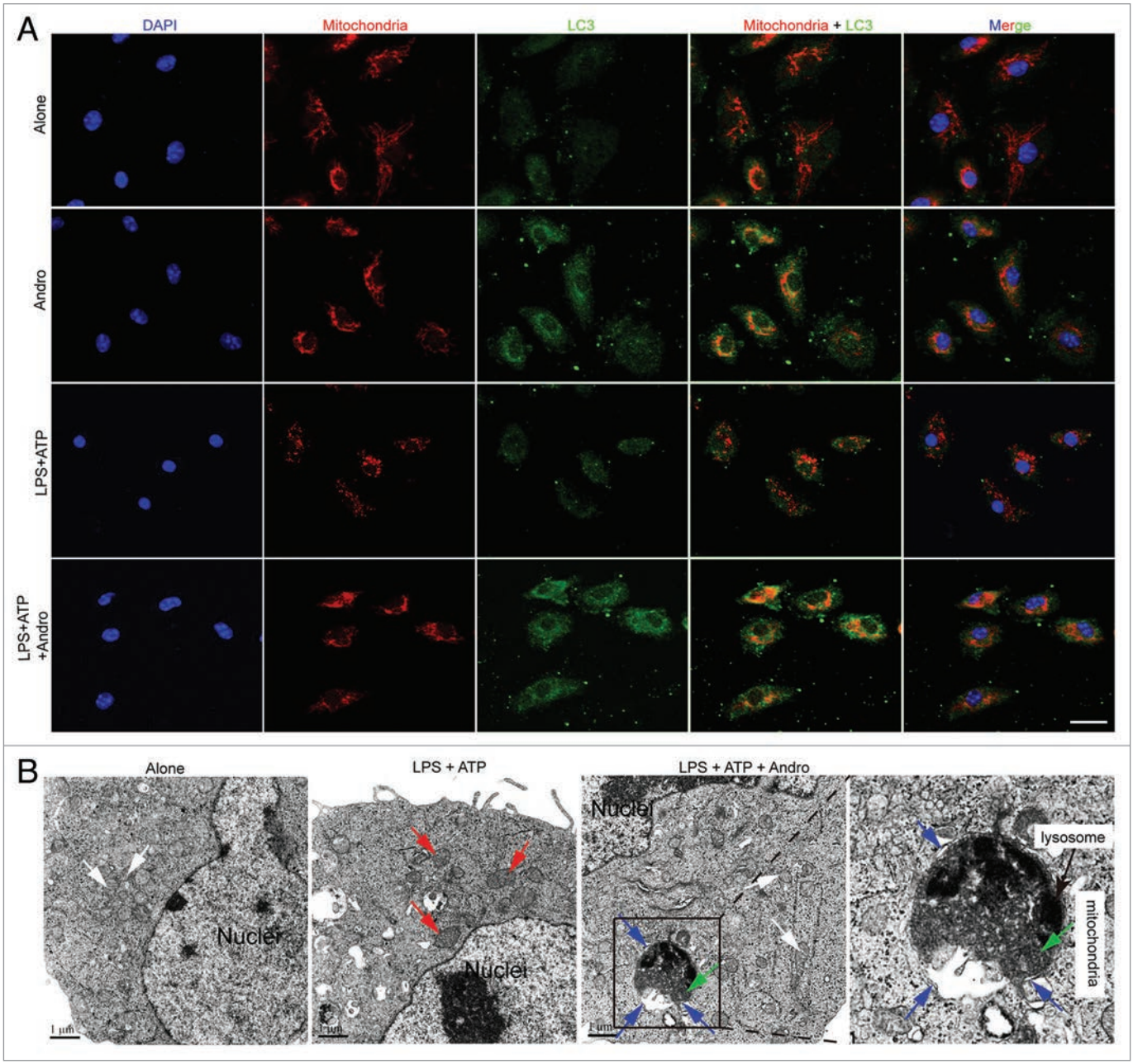

Figure 7. Andrographolide triggers mitophagy in macrophages. (**A**) BMDM cells were cultured with 30 μM Andro for 1 h (Alone and Andro group) or BMDM cells were cultured with 100 ng/ml LPS for 3 h, and then with 30 μM Andro for 1 h, followed by 15 min incubation with 5 mM ATP(LPS+ATP and LPS+ATP+Andro group). LC3 (green) and mitochondria (MitoTracker Red) colocalization were examined by immunofluorescence. Scale bar: 10 μm. (**B**) LPS-primed THP-1 cells were treated with 30 μM Andro for 1 h, followed by 1 h incubation with 5 mM ATP. Cells were collected for transmission electron microscopy assay. White arrow, normal mitochondria; red arrow, swollen mitochondria with disrupted cristae; blue arrow, a double membrane; green arrow, the damaged mitochondria were localized near a lysosome in the autophagolysosome. Data shown in (**A and B**) are representative of 3 experiments. Andro, andrographolide.

These findings suggest that Andro can induce or inhibit autophagy in various kinds of cells via different mechanisms. We speculate that these discrepancies may result from the use of different cell types or different Andro concentrations and incubation times.

In conclusion, our results in this study provide strong evidence for the chemopreventive activity of Andro against colitis-associated colorectal cancer in mice through inhibiting inflammation. The mechanism underlying the activity of Andro involves PIK3CA-AKT1-MTOR-RPS6KB1 pathway-mediated mitophagy-dependent inactivation of the NLRP3 inflammasome, thus leading to decreased NLRP3-PYCARD-CASP1-mediated IL1B secretion from macrophages. Our data presented here may help guide decisions regarding the use of

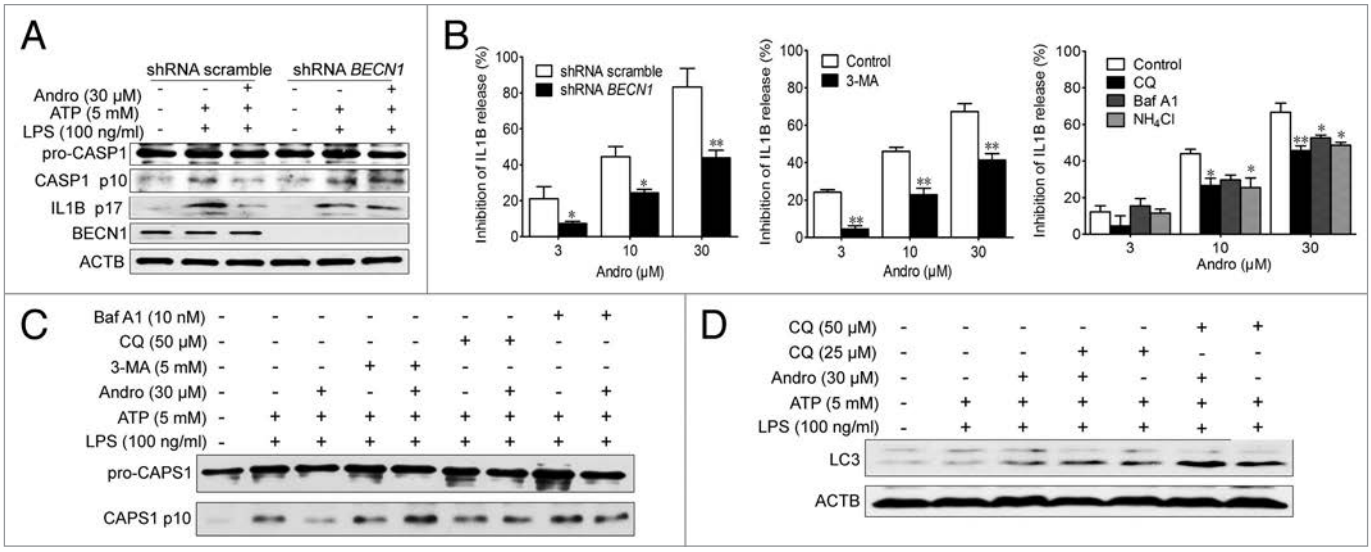

Figure 8. Andro-induced mitophagy is responsible for inhibition of the NLRP3 inflammasome. (**A and B**) THP-1 cells were transfected with control shRNA or shRNA targeting *BECN1*. After 48 h, LPS-primed THP-1 cells were treated with Andro for 1 h, followed by 1 h incubation with 5 mM ATP. The effects of Andro on CASP1 activation (**A**) and IL1B maturation (**B**) were measured by western blotting and ELISA, respectively. **P* < 0.05, ***P* < 0.01 vs. control group. (**B**–**D**) LPS-primed THP-1 cells were incubated with the autophagy inhibitors 3-MA (5 mM), chloroquine (CQ, 25 μM), Baf A1 (10 nM), or NH_4Cl (20 mM) for 1 h, followed by Andro treatment for 1 h, and then stimulated with ATP for 1 h. The effects of Andro on IL1B maturation (**B**), CASP1 activation (**C**), and LC3 expression (**D**) were measured by ELISA and western blotting, respectively. Data shown in (**B**) are mean ± SEM of 3 different experiments. Data shown in (**A, C, and D**) are representative of 3 experiments. Andro, andrographolide.

Andro as an anti-inflammatory agent in IBD patients, ultimately reducing the risk of CAC.

Materials and Methods

Animals

C57BL/6 mice, 6–8 wk old, were purchased from the Model Animal Research Center of Nanjing University (Nanjing, China). They were maintained with free access to pellet food and water in plastic cages at 21 ± 2 °C and kept on a 12 h light/dark cycle. Animal welfare and experimental procedures were performed in accordance with the Guide for the Care and Use of Laboratory Animals (National Institutes of Health, the United States) and the related ethical regulations of our university. All efforts were made to reduce the number of animals used and to minimize animals' suffering.

Cell culture

The human monocytic THP-1 cell line was purchased from the Shanghai Institute of Cell Biology (Shanghai, China) and cultured at 37 °C in a 5% (v/v) CO_2 atmosphere. Peritoneal macrophages were harvested from the peritoneal cavity of C57BL/6 mice and purified by adherence to tissue culture plastic.[56] Bone marrow cells were isolated from C57BL/6 mice and cultured with DMEM supplemented with 10% fetal bovine serum (Gibco, 10100147) and 20 ng/ml recombinant murine M-CSF (PeproTech, 315-02). Culture fluid was exchanged with fresh culture medium every 3 d. Under these conditions, an adherent macrophage monolayer was obtained at d 7. Cells were harvested and seeded on 24-well plates. After culturing for 6 h without M-CSF, the cells were used for the experiments as bone marrow-derived macrophages (BMDM).

Chemicals, reagents, and antibodies

Andrographolide (Andro, 365645), azoxymethane (AOM, A5486), phorbol myristate acetate (PMA, P1585), 3-methyladenine (3-MA, M9281), 4',6-diamidino-2-phenylindole (DAPI, D8417), LPS (L2630), adenosine triphosphate (ATP, A7699), CQ (B1793), and Baf A1 (PHR1258) were purchased from Sigma-Aldrich. Dextran sulfate sodium (DSS, 36–50 K_d, 0216011080) was purchased from MP Biomeicals. Myeloperoxidase (MPO, A044) activity assay kit was purchased from Nanjing Jiancheng Bioengineering Institute. ELISA kits for murine TNF (12-2720), murine IL17A (12-2170), murine IFNG (12-2000), murine IL1B (12-2012) and human IL1B (12-1012) were purchased from Beijing Dakewe Biotech Company Limited. Anti-LC3B (2775), anti-BECN1 (3738), anti-p-MTOR (2971), anti-p-AKT1 (Thr 308, 4056), anti-p-PIK3CA (9275), anti-p-STAT3 (9138), and anti-phospho-MAPK1/3 antibody (Thy202/Tyr204, 9101) were purchased from Cell Signaling Technology. Anti-NLRP3 (3560-1), anti-p-RELA (1546-1), anti-p-RPS6KB1 (1135-1), anti-p-EIF4EBP1 (2411-1) and anti-CASP1 (3345-1) were purchased from Epitomics. Anti-PYCARD (ASC, sc-271054), anti-ACTB (sc-1616), anti-PTGS2/COX2 (sc-19999) and anti-PCNA (sc-56) were purchased from Santa Cruz Biotechnology. JC-1 (T-3168), Alexa Fluor 488 goat anti-rabbit IgG (A11008), and the mitochondrial specific dye MitoTracker Red CMXRos (M7512) were purchased from Invitrogen. Anti-F4/80-PE (130-099-437) and anti-PE MicroBeads (130-048-801) were purchased from Miltenyi. The Mitochondria/Cytosol

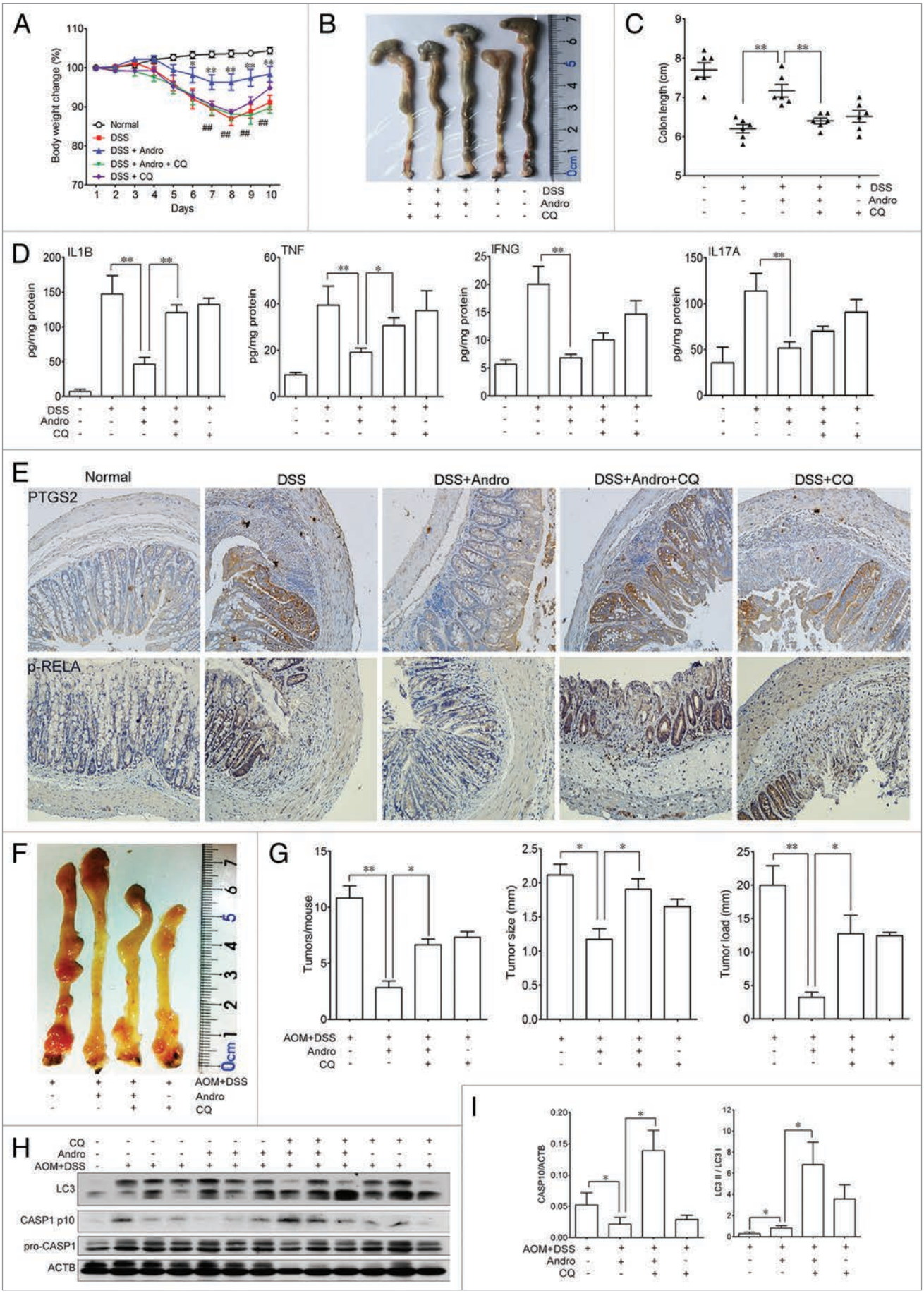

Figure 9 (See opposite page). Andrographolide-driven mitophagy-mediated NLRP3 inflammasome inactivation is responsible for amelioration of murine models for colitis and CAC. (**A–E**) Mice were treated with 2.5% DSS in their drinking water for 7 d to induce colitis. Andro (5 mg/kg) was administered i.p. daily. CQ (50 mg/kg) was administered i.p. every 2 d. Mice were sacrificed on d 10 after colitis induction. Values are mean ± SEM of 6 mice/group. (**A**) The body weight of the mice was measured and presented as a percentage of the original body weight. (**B**) The colon was photographed. (**C**) The length of the colon was measured when the mice were sacrificed. (**D**) Protein levels of various cytokines in colon homogenates from DSS-induced mice at d 10 were examined by ELISA. $^{*}P < 0.05$, $^{**}P < 0.01$. (**E**) Expression of PTGS2/COX2 and p-RELA/p-p65 were examined by immunohistochemical staining of paraffin-embedded colon sections from DSS-induced mice at d 10. (**F–I**) Mice were injected i.p. with a single dose (7.5 mg/kg) of AOM followed by 3 cycles of 2.5% DSS given in the drinking water for 5 d. Andro (15 mg/kg) was given i.g. daily and CQ (50 mg/kg) was i.p. administered every 2 d during the interval between DSS cycles. Mice were sacrificed on d 95 after CAC induction. Values are mean ± SEM of 6 mice/group. (**F**) The inside of the colon was photographed. (**G**) Tumor numbers, size, and load were measured. $^{*}P < 0.05$, $^{**}P < 0.01$. (**H**) Macrophages were isolated from the spleen of AOM-DSS mice on d 95 using commercial magnetic beads as described in Materials and Methods. After stimulation with 5 mM ATP for 30 min, proteins were collected for western blotting. (**I**) Statistical data of the expressions of CASP1 and LC3 from 6 mice were shown. $^{*}P < 0.05$. Andro, andrographolide.

Fractionation Kit (ab65320) was purchased from Abcam. The GTVisin™ anti-mouse/anti-rabbit immunohistochemical analysis kit was purchased from Shanghai Gene Company Ltd. The shRNA scramble and shRNA BECN1 were purchased from Shanghai NeuronBiotech Company. All other chemicals were obtained from Sigma-Aldrich.

Induction and treatment of colitis-associated cancer and colitis

To induce colitis-associated cancer (CAC), mice were injected intraperitoneally (i.p.) with a single dose (7.5 mg/kg) of AOM followed by 3 cycles of 2.5% DSS given in the drinking water for 5 d.[57] Andro was administered through i.g. (intragastrically) daily at the indicated dose during the interval between DSS cycles. Mice were sacrificed on d 95 after CAC induction. The entire colon and rectum were processed for histopathological examination. Acute colitis was induced by giving 2.5% DSS in the drinking water for 7 d. Andro was administered through i.p. injection daily at the indicated dose for 10 d. Body weight, stool consistency, and the presence of gross blood in feces and at the anus were observed every day. The disease activity index was calculated by assigning well-established and validated scores. Briefly, the following parameters were used for calculation: a) diarrhea (0 points = normal, 2 points = loose stools, 4 points = watery diarrhea); b) hematochezia (0 points = no bleeding, 2 points = slight bleeding, 4 points = gross bleeding).

Histological analysis, immunohistochemistry, and immunofluorescence

Colonic sections from mice were obtained for H&E staining and analyzed by a pathologist using a light microscope (Olympus). For immunohistochemistry or immunofluorescence staining, the sections were deparaffinized, rehydrated, and washed in 1% PBS-Tween 20, and then treated with 2% hydrogen peroxide, blocked with 3% goat serum (Life Technology, 16210-064) and incubated for 2 h at room temperature with specific primary antibodies. For immunofluorescence of ITGAM/CD11b, the slides were incubated with ITGAM-FITC (eBioscience, 11-0112) for 1 h and then counter-stained with DAPI for 5 min. For immunofluorescence of LC3, the protocol has been reported previously.[58] For immunohistochemistry, the slides were incubated with streptavidin-HRP (Shanghai Gene Company, GK500705) for 40 min, then stained with DAB (Shanghai Gene Company, GK500705) substrate and counter-stained with hematoxylin. Images were acquired by confocal laser-scanning microscopy (Olympus FV1000).

Cytokine analysis by ELISA

Colons from mice in each group were homogenized with lysis buffer to extract total protein. The homogenate was centrifuged at 12 000 *g* at 4 °C for 15 min. The amount of total extracted protein was determined by BCA™ protein assay kit (Pierce, 23225). The commercial ELISA kits (Dakewe, Beijing) of murine IFNG (12-2000), murine IL17A (12-2170), murine TNF (12-2720), murine IL1B (12-2012) and human IL1B (12-1012) were used to measure the cytokine levels.

Real-time PCR

Real-time PCR was performed as follows: RNA samples were reverse transcribed to cDNA and subjected to quantitative PCR, which was performed with the BioRad Real-Time PCR Detection System (Bio-Rad, CFX Connect™) using iQ™ SYBR® Green Supermix (Bio-Rad, 1708880), and threshold cycle numbers were obtained using BioRad CFX Manager software. The program for amplification was 1 cycle of 95 °C for 2 min followed by 40 cycles of 95 °C for 10 s, 60 °C for 30 s, and 95 °C for 10 s. The primer sequences used in this study are listed in the Supplementary data.

Western blot and transmission electron microscopy assay

The protocols for western blot and transmission electron microscopy assay have been reported previously.[58]

Coimmunoprecipitation assay

Cells were collected and lysized with lysis buffer (Beyotime company, P0013) on ice for 30 min and centrifuged at 12,000 *g* at 4 °C for 15 min. The supernatant fractions were collected and incubated with 1 μg of appropriate antibody at 4 °C overnight and precipitated with protein A/G-agarose beads (Santa Cruz, sc-2003) for another 4 h at 4 °C. The beads were washed with the lysis buffer 4 times by centrifugation at 1,000 *g* at 4 °C. The immunoprecipitated proteins were separated by SDS-PAGE and western blot was performed with the indicated antibodies.

Statistical analysis

Data are expressed as mean ± SEM. Student's *t* test and one-way ANOVA test were used for statistical analyses of the data. Cases in which *P* values were < 0.05 or < 0.01 were considered statistically significant.

Disclosure of Potential Conflicts of Interest

No potential conflicts of interest were disclosed.

Acknowledgments

This work was supported by Science Fund for Creative Research Groups of NSFC (No. 81121062), National Natural Science Foundation of China (Nos. 91229109, 81330079, 90913023, 91129728), National Science and Technology Major Project (No. 2012ZX09304-001), and Jiangsu Province Clinical Science and Technology Project (Clinical Research Center, BL2012008).

Supplemental Materials

Supplemental materials may be found here:
www.landesbioscience.com/journals/autophagy/article/28374

References

1. Jemal A, Bray F, Center MM, Ferlay J, Ward E, Forman D. Global cancer statistics. CA Cancer J Clin 2011; 61:69-90; PMID:21296855; http://dx.doi.org/10.3322/caac.20107
2. Weir HK, Thun MJ, Hankey BF, Ries LA, Howe HL, Wingo PA, Jemal A, Ward E, Anderson RN, Edwards BK. Annual report to the nation on the status of cancer, 1975-2000, featuring the uses of surveillance data for cancer prevention and control. J Natl Cancer Inst 2003; 95:1276-99; PMID:12953083; http://dx.doi.org/10.1093/jnci/djg040
3. Fearon ER. Molecular genetics of colorectal cancer. Annu Rev Pathol 2011; 6:479-507; PMID:21090969; http://dx.doi.org/10.1146/annurev-pathol-011110-130235
4. Pancione M, Remo A, Colantuoni V. Genetic and epigenetic events generate multiple pathways in colorectal cancer progression. Patholog Res Int 2012; 2012:509348; PMID:22888469; http://dx.doi.org/10.1155/2012/509348
5. Grivennikov SI. Inflammation and colorectal cancer: colitis-associated neoplasia. Semin Immunopathol 2013; 35:229-44; PMID:23161445; http://dx.doi.org/10.1007/s00281-012-0352-6
6. Rogler G. Inflammatory bowel disease cancer risk, detection and surveillance. Dig Dis 2012; 30(Suppl 2):48-54; PMID:23207932; http://dx.doi.org/10.1159/000341893
7. Colotta F, Allavena P, Sica A, Garlanda C, Mantovani A. Cancer-related inflammation, the seventh hallmark of cancer: links to genetic instability. Carcinogenesis 2009; 30:1073-81; PMID:19468060; http://dx.doi.org/10.1093/carcin/bgp127
8. Hanahan D, Weinberg RA. Hallmarks of cancer: the next generation. Cell 2011; 144:646-74; PMID:21376230; http://dx.doi.org/10.1016/j.cell.2011.02.013
9. Terzić J, Grivennikov S, Karin E, Karin M. Inflammation and colon cancer. Gastroenterology 2010; 138:2101-14, e5; PMID:20420949; http://dx.doi.org/10.1053/j.gastro.2010.01.058
10. Fantini MC, Pallone F. Cytokines: from gut inflammation to colorectal cancer. Curr Drug Targets 2008; 9:375-80; PMID:18473765; http://dx.doi.org/10.2174/138945008784221206
11. Bernstein CN, Blanchard JF, Kliewer E, Wajda A. Cancer risk in patients with inflammatory bowel disease: a population-based study. Cancer 2001; 91:854-62; PMID:11241255; http://dx.doi.org/10.1002/1097-0142(20010215)91:4<854::AID-CNCR1073>3.0.CO;2-Z
12. Triantafillidis JK, Nasioulas G, Kosmidis PA. Colorectal cancer and inflammatory bowel disease: epidemiology, risk factors, mechanisms of carcinogenesis and prevention strategies. Anticancer Res 2009; 29:2727-37; PMID:19596953
13. Farrell RJ, Peppercorn MA. Ulcerative colitis. Lancet 2002; 359:331-40; PMID:11830216; http://dx.doi.org/10.1016/S0140-6736(02)07499-8
14. Gross O, Thomas CJ, Guarda G, Tschopp J. The inflammasome: an integrated view. Immunol Rev 2011; 243:136-51; PMID:21884173; http://dx.doi.org/10.1111/j.1600-065X.2011.01046.x
15. Nunes T, de Souza HS. Inflammasome in intestinal inflammation and cancer. Mediators Inflamm 2013; 2013:654963; PMID:23606794; http://dx.doi.org/10.1155/2013/654963
16. Ding WX, Yin XM. Mitophagy: mechanisms, pathophysiological roles, and analysis. Biol Chem 2012; 393:547-64; PMID:22944659; http://dx.doi.org/10.1515/hsz-2012-0119
17. Lupfer C, Thomas PG, Anand PK, Vogel P, Milasta S, Martinez J, Huang G, Green M, Kundu M, Chi H, et al. Receptor interacting protein kinase 2-mediated mitophagy regulates inflammasome activation during virus infection. Nat Immunol 2013; 14:480-8; PMID:23525089; http://dx.doi.org/10.1038/ni.2563
18. Wiart C, Kumar K, Yusof MY, Hamimah H, Fauzi ZM, Sulaiman M. Antiviral properties of ent-labdene diterpenes of Andrographis paniculata nees, inhibitors of herpes simplex virus type 1. Phytother Res 2005; 19:1069-70; PMID:16372376; http://dx.doi.org/10.1002/ptr.1765
19. Abu-Ghefreh AA, Canatan H, Ezeamuzie CI. In vitro and in vivo anti-inflammatory effects of andrographolide. Int Immunopharmacol 2009; 9:313-8; PMID:19110075; http://dx.doi.org/10.1016/j.intimp.2008.12.002
20. Chan SJ, Wong WS, Wong PT, Bian JS. Neuroprotective effects of andrographolide in a rat model of permanent cerebral ischaemia. Br J Pharmacol 2010; 161:668-79; PMID:20880404; http://dx.doi.org/10.1111/j.1476-5381.2010.00906.x
21. Rajagopal S, Kumar RA, Deevi DS, Satyanarayana C, Rajagopalan R. Andrographolide, a potential cancer therapeutic agent isolated from Andrographis paniculata. J Exp Ther Oncol 2003; 3:147-58; PMID:14641821; http://dx.doi.org/10.1046/j.1359-4117.2003.01090.x
22. Ricciotti E, FitzGerald GA. Prostaglandins and inflammation. Arterioscler Thromb Vasc Biol 2011; 31:986-1000; PMID:21508345; http://dx.doi.org/10.1161/ATVBAHA.110.207449
23. Jobin C, Sartor RB. NF-kappaB signaling proteins as therapeutic targets for inflammatory bowel diseases. Inflamm Bowel Dis 2000; 6:206-13; PMID:10961593; http://dx.doi.org/10.1097/00054725-200008000-00007
24. Shimada K, Crother TR, Karlin J, Dagvadorj J, Chiba N, Chen S, Ramanujan VK, Wolf AJ, Vergnes L, Ojcius DM, et al. Oxidized mitochondrial DNA activates the NLRP3 inflammasome during apoptosis. Immunity 2012; 36:401-14; PMID:22342844; http://dx.doi.org/10.1016/j.immuni.2012.01.009
25. Zhou R, Yazdi AS, Menu P, Tschopp J. A role for mitochondria in NLRP3 inflammasome activation. Nature 2011; 469:221-5; PMID:21124315; http://dx.doi.org/10.1038/nature09663
26. Nathan C, Ding A. Nonresolving inflammation. Cell 2010; 140:871-82; PMID:20303877; http://dx.doi.org/10.1016/j.cell.2010.02.029
27. Ligumsky M, Simon PL, Karmeli F, Rachmilewitz D. Role of interleukin 1 in inflammatory bowel disease--enhanced production during active disease. Gut 1990; 31:686-9; PMID:2379873; http://dx.doi.org/10.1136/gut.31.6.686
28. Gionchetti P, Campieri M, Belluzzi A, Boni P, Brignola C, Ferretti H, Iannone P, Miglioli M, Barbara L. Interleukin 1 in ulcerative colitis. Gut 1991; 32:338; PMID:2013435; http://dx.doi.org/10.1136/gut.32.3.338-a
29. Reinecker HC, Steffen M, Witthoeft T, Pflueger I, Schreiber S, MacDermott RP, Raedler A. Enhanced secretion of tumour necrosis factor-alpha, IL-6, and IL-1 beta by isolated lamina propria mononuclear cells from patients with ulcerative colitis and Crohn's disease. Clin Exp Immunol 1993; 94:174-81; PMID:8403503; http://dx.doi.org/10.1111/j.1365-2249.1993.tb05997.x
30. McAlindon ME, Hawkey CJ, Mahida YR. Expression of interleukin 1 β and interleukin 1 β converting enzyme by intestinal macrophages in health and inflammatory bowel disease. Gut 1998; 42:214-9; PMID:9536946; http://dx.doi.org/10.1136/gut.42.2.214
31. Coccia M, Harrison OJ, Schiering C, Asquith MJ, Becher B, Powrie F, Maloy KJ. IL-1β mediates chronic intestinal inflammation by promoting the accumulation of IL-17A secreting innate lymphoid cells and CD4(+) Th17 cells. J Exp Med 2012; 209:1595-609; PMID:22891275; http://dx.doi.org/10.1084/jem.20111453
32. Dinarello CA. Biologic basis for interleukin-1 in disease. Blood 1996; 87:2095-147; PMID:8630372
33. Ben-Sasson SZ, Hu-Li J, Quiel J, Cauchetaux S, Ratner M, Shapira I, Dinarello CA, Paul WE. IL-1 acts directly on CD4 T cells to enhance their antigen-driven expansion and differentiation. Proc Natl Acad Sci U S A 2009; 106:7119-24; PMID:19359475; http://dx.doi.org/10.1073/pnas.0902745106
34. Sutton C, Brereton C, Keogh B, Mills KH, Lavelle EC. A crucial role for interleukin (IL)-1 in the induction of IL-17-producing T cells that mediate autoimmune encephalomyelitis. J Exp Med 2006; 203:1685-91; PMID:16818675; http://dx.doi.org/10.1084/jem.20060285
35. Martinon F, Burns K, Tschopp J. The inflammasome: a molecular platform triggering activation of inflammatory caspases and processing of proIL-beta. Mol Cell 2002; 10:417-26; PMID:12191486; http://dx.doi.org/10.1016/S1097-2765(02)00599-3
36. Zaki MH, Boyd KL, Vogel P, Kastan MB, Lamkanfi M, Kanneganti TD. The NLRP3 inflammasome protects against loss of epithelial integrity and mortality during experimental colitis. Immunity 2010; 32:379-91; PMID:20303296; http://dx.doi.org/10.1016/j.immuni.2010.03.003
37. Allen IC, TeKippe EM, Woodford RM, Uronis JM, Holl EK, Rogers AB, Herfarth HH, Jobin C, Ting JP. The NLRP3 inflammasome functions as a negative regulator of tumorigenesis during colitis-associated cancer. J Exp Med 2010; 207:1045-56; PMID:20385749; http://dx.doi.org/10.1084/jem.20100050
38. Bauer C, Duewell P, Mayer C, Lehr HA, Fitzgerald KA, Dauer M, Tschopp J, Endres S, Latz E, Schnurr M. Colitis induced in mice with dextran sulfate sodium (DSS) is mediated by the NLRP3 inflammasome. Gut 2010; 59:1192-9; PMID:20442201; http://dx.doi.org/10.1136/gut.2009.197822
39. Arai Y, Takanashi H, Kitagawa H, Okayasu I. Involvement of interleukin-1 in the development of ulcerative colitis induced by dextran sulfate sodium in mice. Cytokine 1998; 10:890-6; PMID:9878126; http://dx.doi.org/10.1006/cyto.1998.0355
40. Siegmund B, Lehr H-A, Fantuzzi G, Dinarello CA. IL-1 β -converting enzyme (caspase-1) in intestinal inflammation. Proc Natl Acad Sci U S A 2001; 98:13249-54; PMID:11606779; http://dx.doi.org/10.1073/pnas.231473998

41. Bauer C, Duewell P, Lehr HA, Endres S, Schnurr M. Protective and aggravating effects of Nlrp3 inflammasome activation in IBD models: influence of genetic and environmental factors. Dig Dis 2012; 30(Suppl 1):82-90; PMID:23075874; http://dx.doi.org/10.1159/000341681
42. Siegmund B, Fantuzzi G, Rieder F, Gamboni-Robertson F, Lehr HA, Hartmann G, Dinarello CA, Endres S, Eigler A. Neutralization of interleukin-18 reduces severity in murine colitis and intestinal IFN-gamma and TNF-alpha production. Am J Physiol Regul Integr Comp Physiol 2001; 281:R1264-73; PMID:11557635
43. Sivakumar PV, Westrich GM, Kanaly S, Garka K, Born TL, Derry JM, Viney JL. Interleukin 18 is a primary mediator of the inflammation associated with dextran sulphate sodium induced colitis: blocking interleukin 18 attenuates intestinal damage. Gut 2002; 50:812-20; PMID:12010883; http://dx.doi.org/10.1136/gut.50.6.812
44. Bauer C, Loher F, Dauer M, Mayer C, Lehr HA, Schönharting M, Hallwachs R, Endres S, Eigler A. The ICE inhibitor pralnacasan prevents DSS-induced colitis in C57BL/6 mice and suppresses IP-10 mRNA but not TNF-alpha mRNA expression. Dig Dis Sci 2007; 52:1642-52; PMID:17393315; http://dx.doi.org/10.1007/s10620-007-9802-8
45. Loher F, Bauer C, Landauer N, Schmall K, Siegmund B, Lehr HA, Dauer M, Schoenharting M, Endres S, Eigler A. The interleukin-1 beta-converting enzyme inhibitor pralnacasan reduces dextran sulfate sodium-induced murine colitis and T helper 1 T-cell activation. J Pharmacol Exp Ther 2004; 308:583-90; PMID:14610233; http://dx.doi.org/10.1124/jpet.103.057059
46. Thomas TK, Will PC, Srivastava A, Wilson CL, Harbison M, Little J, Chesonis RS, Pignatello M, Schmolze D, Symington J, et al. Evaluation of an interleukin-1 receptor antagonist in the rat acetic acid-induced colitis model. Agents Actions 1991; 34:187-90; PMID:1838896; http://dx.doi.org/10.1007/BF01993274
47. Coll RC, O'Neill LA. The cytokine release inhibitory drug CRID3 targets ASC oligomerisation in the NLRP3 and AIM2 inflammasomes. PLoS One 2011; 6:e29539; PMID:22216309; http://dx.doi.org/10.1371/journal.pone.0029539
48. Lee KC, Chang HH, Chung YH, Lee TY. Andrographolide acts as an anti-inflammatory agent in LPS-stimulated RAW264.7 macrophages by inhibiting STAT3-mediated suppression of the NF-κB pathway. J Ethnopharmacol 2011; 135:678-84; PMID:21497192; http://dx.doi.org/10.1016/j.jep.2011.03.068
49. Hsieh CY, Hsu MJ, Hsiao G, Wang YH, Huang CW, Chen SW, Jayakumar T, Chiu PT, Chiu YH, Sheu JR. Andrographolide enhances nuclear factor-kappaB subunit p65 Ser536 dephosphorylation through activation of protein phosphatase 2A in vascular smooth muscle cells. J Biol Chem 2011; 286:5942-55; PMID:21169355; http://dx.doi.org/10.1074/jbc.M110.123968
50. Martinon F. Dangerous liaisons: mitochondrial DNA meets the NLRP3 inflammasome. Immunity 2012; 36:313-5; PMID:22444626; http://dx.doi.org/10.1016/j.immuni.2012.03.005
51. Kepp O, Galluzzi L, Kroemer G. Mitochondrial control of the NLRP3 inflammasome. Nat Immunol 2011; 12:199-200; PMID:21321591; http://dx.doi.org/10.1038/ni0311-199
52. Schroder K, Tschopp J. The inflammasomes. Cell 2010; 140:821-32; PMID:20303873; http://dx.doi.org/10.1016/j.cell.2010.01.040
53. Nakahira K, Haspel JA, Rathinam VA, Lee SJ, Dolinay T, Lam HC, Englert JA, Rabinovitch M, Cernadas M, Kim HP, et al. Autophagy proteins regulate innate immune responses by inhibiting the release of mitochondrial DNA mediated by the NALP3 inflammasome. Nat Immunol 2011; 12:222-30; PMID:21151103; http://dx.doi.org/10.1038/ni.1980
54. Chen W, Feng L, Nie H, Zheng X. Andrographolide induces autophagic cell death in human liver cancer cells through cyclophilin D-mediated mitochondrial permeability transition pore. Carcinogenesis 2012; 33:2190-8; PMID:22869602; http://dx.doi.org/10.1093/carcin/bgs264
55. Zhou J, Hu SE, Tan SH, Cao R, Chen Y, Xia D, Zhu X, Yang XF, Ong CN, Shen HM. Andrographolide sensitizes cisplatin-induced apoptosis via suppression of autophagosome-lysosome fusion in human cancer cells. Autophagy 2012; 8:338-49; PMID:22302005; http://dx.doi.org/10.4161/auto.18721
56. Malik M, Jividen K, Padmakumar VC, Cataisson C, Li L, Lee J, Howard OM, Yuspa SH. Inducible NOS-induced chloride intracellular channel 4 (CLIC4) nuclear translocation regulates macrophage deactivation. Proc Natl Acad Sci U S A 2012; 109:6130-5; PMID:22474389; http://dx.doi.org/10.1073/pnas.1201351109
57. Wirtz S, Neufert C, Weigmann B, Neurath MF. Chemically induced mouse models of intestinal inflammation. Nat Protoc 2007; 2:541-6; PMID:17406617; http://dx.doi.org/10.1038/nprot.2007.41
58. Guo WJ, Zhang YM, Zhang L, Huang B, Tao FF, Chen W, Guo ZJ, Xu Q, Sun Y. Novel monofunctional platinum (II) complex Mono-Pt induces apoptosis-independent autophagic cell death in human ovarian carcinoma cells, distinct from cisplatin. Autophagy 2013; 9:996-1008; PMID:23580233; http://dx.doi.org/10.4161/auto.24407